

Video Article

Light-sheet Fluorescence Microscopy to Capture 4-Dimensional Images of the Effects of Modulating Shear Stress on the Developing Zebrafish Heart

Victoria Messerschmidt^{*1}, Zachary Bailey^{*1}, Kyung In Baek², Yichen Ding², Jeffrey J. Hsu², Richard Bryant¹, Rongsong Li³, Tzung K. Hsiai², Juhyun Lee¹

¹Department of Bioengineering, The University of Texas at Arlington

²Department of Medicine (Cardiology) and Bioengineering, UCLA

³College of Health Science and Environmental Engineering, Shenzhen Technology University

*These authors contributed equally

Correspondence to: Juhyun Lee at juhyun.lee@uta.edu

URL: <https://www.jove.com/video/57763>

DOI: [doi:10.3791/57763](https://doi.org/10.3791/57763)

Keywords: Bioengineering, Issue 138, Selective plane illumination microscopy, Notch signaling, trabeculation, hemodynamics, zebrafish, cardiac development, shear stress, 4-Dimensional heart imaging, mechanobiology, heart, light sheet fluorescence microscopy

Date Published: 8/10/2018

Citation: Messerschmidt, V., Bailey, Z., Baek, K.I., Ding, Y., Hsu, J.J., Bryant, R., Li, R., Hsiai, T.K., Lee, J. Light-sheet Fluorescence Microscopy to Capture 4-Dimensional Images of the Effects of Modulating Shear Stress on the Developing Zebrafish Heart. *J. Vis. Exp.* (138), e57763, doi:10.3791/57763 (2018).

Abstract

The hemodynamic forces experienced by the heart influence cardiac development, especially trabeculation, which forms a network of branching outgrowths from the myocardium. Genetic program defects in the Notch signaling cascade are involved in ventricular defects such as Left Ventricular Non-Compaction Cardiomyopathy or Hypoplastic Left Heart Syndrome. Using this protocol, it can be determined that shear stress driven trabeculation and Notch signaling are related to one another. Using Light-sheet Fluorescence Microscopy, visualization of the developing zebrafish heart was possible. In this manuscript, it was assessed whether hemodynamic forces modulate the initiation of trabeculation via Notch signaling and thus, influence contractile function occurs. For qualitative and quantitative shear stress analysis, 4-D (3-D+time) images were acquired during zebrafish cardiac morphogenesis, and integrated light-sheet fluorescence microscopy with 4-D synchronization captured the ventricular motion. Blood viscosity was reduced via *gata1a*-morpholino oligonucleotides (MO) micro-injection to decrease shear stress, thereby, down-regulating Notch signaling and attenuating trabeculation. Co-injection of *Nrg1* mRNA with *gata1a* MO rescued Notch-related genes to restore trabeculation. To confirm shear stress driven Notch signaling influences trabeculation, cardiomyocyte contraction was further arrested via *tnnt2a*-MO to reduce hemodynamic forces, thereby, down-regulating Notch target genes to develop a non-trabeculated myocardium. Finally, corroboration of the expression patterns of shear stress-responsive Notch genes was conducted by subjecting endothelial cells to pulsatile flow. Thus, the 4-D light-sheet microscopy uncovered hemodynamic forces underlying Notch signaling and trabeculation with clinical relevance to non-compaction cardiomyopathy.

Video Link

The video component of this article can be found at <https://www.jove.com/video/57763/>

Introduction

Biomechanical forces, such as hemodynamic shear stress, are intimately involved in cardiac morphogenesis. In response to hemodynamic shear forces, myocardial ridges and grooves develop in a wave-like trabecular network in alignment with the direction of the shear stress across the atrioventricular (AV) valve¹. Cardiac trabeculation is necessary to increase contractile function and myocardial mass². Mutations in Notch signaling pathways result in congenital heart defects in humans and other vertebrates³. For example, *gata1a*⁴ and *tnnt2a*⁵ morpholino oligonucleotides (MO) have been shown to reduce erythropoiesis, while erythropoietin mRNA (EPO)⁶ and Isoproterenol (ISO)⁷ increase red blood cells and heart rate respectively, and therefore wall shear stress (WSS). Furthermore, ErbB2 signaling, downstream of Notch, promotes cardiomyocyte proliferation and differentiation to generate contractile force, which in turn activates Notch signaling^{8,9}. It is suggested that shear stress governs Notch signaling driven trabeculation for ventricular development. Currently, there are many studies that attempt to further understand the genetic programming events leading to congenital heart defects (CHD)^{10,11,12}, but very little are investigating how mechanical forces influence the forming heart.

In order to investigate the mechanical forces acting on the endocardium, close observation during the developmental period needs to be implemented. However, it is challenging to obtain good quality images of *in vivo* beating samples due to the inherence of traditional microscopy¹³. In order to observe the development over time within a sample, physical sectioning and staining, therefore, need to occur^{13,14,15}. Although confocal microscopy is widely used to image the 3-D structure of samples^{14,16}, these imaging systems' acquisition is still limited by slow scanning speeds.

Light-sheet fluorescence microscopy (LSFM) is a unique imaging technique that allows the visualization of *in vivo* dynamic events with long working distance¹³. This technique uses a light-sheet fluorescent microscopy to optically section a sample¹⁷. Due to illumination of only a thin sheet of light on the sample, there is a reduction in photo-bleaching and photo toxicity^{13,18}. The large field of view and long working distance allows for large samples to stay intact as they are imaged^{13,14,17}. The low magnification allows for a larger area to be imaged, while the long working distance allows for thicker samples to be imaged without compromising the signal-to-noise ratio. Many groups have used LSFM to image entire embryos¹⁷, brains^{14,18}, muscles and hearts¹⁹ among other tissues, showing the diverse types of samples that can be imaged.

Although previous research demonstrated reduced hemodynamic shear force by occluding the inflow or outflow tracks of the zebrafish heart, the information is solely qualitative. It results in an abnormal third chamber, diminished cardiac looping, and impaired valve formation²⁰. The 4-D LSFM images give a new perspective into the way the hemodynamic shear forces affect the development of the cardiac tissue. These mechanical forces may activate force-sensitive signaling molecules and induce the formation of the trabecular ridges. Because of the added time aspect of 4-D imaging, one is able to track changes in development in real time, which could lead to new revelations that had gone unnoticed previously. The zebrafish is an ideal model for imaging because scientists can observe an entire vertebrate animal versus only cell-cell interactions. Oxygen can also diffuse through the entire embryo, which allows development to occur without depending on the vascular system, unlike in mammalian development. Even though the zebrafish heart lacks the pulmonary organs, which require a four-chambered heart, there is a large number of cardiac genes that are conserved between zebrafish and humans²¹.

In this manuscript, we describe how to use light-sheet fluorescence microscopy to image the developing trabeculae in zebrafish hearts under various circumstances. First, injection of *gata1a*⁴ or *tnnt2a*⁵ MOs were used to lower the blood viscosity, and therefore WSS. The morphology of the heart was then recorded. In a separate group of fish, we increased the WSS by administering *EPO* mRNA⁶ or isoproterenol⁷ and observed the results. We also conducted a cell study with different pulsatile or oscillatory flow rates. After imaging each group, we found that WSS sensed by the endocardium via Notch signaling initiates trabeculation.

Protocol

The following methods were performed in compliance with UTA and UCLA IACUC protocols. These experimental groups were used with transgenic *Tg(cmlc2:gfp)*, the *wea* (weak atrium) or *clo* (cloche) mutants: (a) wild-type (WT) control, (b) *gata1a* MO, and (c) *tnnt2a* MO injections (Table 1).

Model	Name	Modified Genes	Phenotype	Reference
Control	Wild type	None	N/A	
	Tg(cmlc2:gfp)	Cardiac myosin light chain	Green fluorescence specifically expressed in the myocardium	34
Decreased Wall Shear Stress	Weak atrium (<i>wea</i>) mutant	Atrium-specific myosin heavy chain	Atrium cannot contract, compact ventricle, thick myocardial wall, narrow lumen, dilated atrium,	37
	Cloche (<i>clo</i>) mutant	N/A	Complete removal of endocardium, unnaturally large atrium with small ventricle, nonexistent cardiac cushions	41
	<i>gata1a</i> MO	<i>gata1a</i>	Anemia from lack of red blood cells	4
	<i>tnnt2a</i> MO	<i>tnnt2a</i>		39
Increased Wall Shear Stress	<i>EPO</i> mRNA	None	Severe polycythemia, increase in number of circulating blood cells, increased viscosity	6
	Isoproterenol	None	Increased cardiac rate	7

Table 1: Zebrafish descriptions. Definitions and descriptions of Zebrafish used in experiments.

1. Study Setup

1. Prepare *Nrg1* and *EPO* mRNA for trabeculation rescue.

1. Obtain Human *Nrg1* cDNA and amplify from a donor plasmid.

Note: The Human *Nrg1* cDNA was gifted from William Talbot from Stanford University.

1. Take out necessary reagents and materials, namely PCR mastermix (stored in -20 °C), primers (See Table 2) (stored in -20 °C), a PCR plate (stored at room temperature), and a 20 µL pipette (stored at room temperature). See Table of Materials for example products.

hNrg1-Clone	Forward	TCTTTTTCAGGATCCACCATGGAGATTATTCCCCAGACATGTCTG
	Backward	GAGAGGCCTTGAATTCCTATTAGGCAGAGACAGAAAGGGAGTG

Table 2: Primers for human *Nrg1* cloning.

2. Prepare the mastermix for each primer set in triplicate using the 20 μ L pipette. For 1 set of triplicates, use 37.5 μ L of the mastermix, 3 μ L of DNA-free water, 4.5 μ L of primer. For more triplicates, simply multiply by the number of samples.
 3. Dilute the working solution Human *Nrg1* cDNA (20 ng/ μ g concentration) in the primer strip with DNA-free water so that there is 10 μ L total per well per sample.
Note: Ensure that each solution under step 1.1.1 is evenly distributed. Do this by mixing each solution by pipetting up and down. To prevent cross-contamination, use one pipette tip for only one sample.
 4. Aliquot the *Nrg1* cDNA with the 10 μ L multi-channel pipette to desired wells in the PCR plate.
 5. Add 14.5 μ L of the mastermix to the cDNA in the wells. Apply a sticky cover to the PCR plate to seal the wells, and place into the PCR machine.
 6. Start the PCR machine and ensure that the cycle reaches appropriate temperatures according to the enzymes and primers used.
2. Clone the *Nrg1* cDNA into the plasmid pCS2⁺ at the BamHI and EcoRI sites using excess enzymes BamHI and EcoRI to ensure cDNA is ligated in all plasmids.
 1. Mix the *Nrg1* cDNA with the donor plasmid pCS2⁺, commercially available master mix solution and primers (**Table 2**).
Note: The total reaction volume should be 50 μ L with 25 μ L of master mix, 3 μ L of primers and 1 μ L of 20 ng/ μ L donor plasmid with *Nrg1* cDNA.
 2. Place the mix from step 1.1.2.1 in the PCR machine and set the parameters to meet the following specifications: 98 °C for 10 s, 55 °C for 5 or 15 s, and 72 °C for 5 s/kb.
 3. Purify the PCR product using a purification kit following the manufacturer's instructions. Elute the product into 50 μ L of elution buffer.
 4. Digest the purified PCR product and 5 μ g of pCS2⁺ with BamHI and EcoRI separately at 37 °C for 2 h in a 200 μ L reaction volume. Purify the resulting digestion with a commercial kit and elute in 20 μ L and 100 μ L of Tris-HCl (pH 8.5), respectively.
 5. Ligate 4 μ L of *Nrg1* cDNA and 2 μ L of the digested pCS2⁺ plasmid in a 25 μ L reaction with 1 μ L of a ligase catalyst at 16 °C overnight.
Note: The procedure can be stopped here for overnight incubation.
 6. Use 2 μ L of the ligation solution from step 1.1.2.5 and transform into 50 μ L of *E. coli* bacteria cells suitable for cloning (see **Table of Materials**).
 3. Confirm that the transformation took place by screening the *Nrg1* cDNA clones using PCR. Choose clones at random and add to a solution of specific primers, polymerase, and deoxyribonucleotide triphosphates (dNTPs).
Note: The controls were the vector (pCS2⁺) with and without the insert (human cDNA). Do not pick too big of a colony because excessive bacteria can inhibit PCR.
 1. Pick 8 colonies from the transformation and screen pCS2⁺-*Nrg1* clones using the PCR primers from **Table 2**.
 2. Culture one clone with *Nrg1* cDNA to isolate the pCS2⁺-*Nrg1* plasmid DNA. Inoculate with 100 μ L of *E. coli* bacteria with pCS2⁺-*Nrg1* plasmid into 100 mL of LB media, and culture by shaking (160 - 225 RPM) at 37 °C.
 4. Transfect purified pCS2⁺-*Nrg1* plasmid into HEK-293 cells in a 6-well plate using a commercial transfection reagent following the manufacturer's instructions.
 5. 24 h after transfection, lyse the cells using a lysis buffer and run through an SDS-PAGE gel, transfer to a gel membrane, and then stain with anti-*Nrg1* antibody²². Verify *Nrg1* protein expression using a Western Blot.
Note: The control is an empty pCS2⁺ plasmid. Can be paused here if gel membrane transfer occurs overnight.
 6. Synthesize *Nrg1* mRNA using a commercial product similar to that in the **Table of Materials** and follow the manufacturer's instructions.
 1. Take 5 μ L of the pCS2⁺-*Nrg1* DNA from the bacteria isolated culture, and digest with NotI in a 200 μ L reaction for 2 h at 37 °C to linearize the plasmid.
 2. Purify the linearized plasmid with a commercial kit and elute in 20 μ L of Tris-HCl (pH 8.5).
 3. Conduct *in vitro* transcription with a commercial RNA isolation kit in a 20 μ L reaction using 5 μ L of the linearized plasmid following the manufacturer's instructions.
 4. Add the *in vitro* transcribed *Nrg1* to 350 μ L of RNA lysis buffer and then purify with an RNA isolation kit. Elute the RNA into 60 μ L of Tris-HCl (pH 8.5).
 5. Measure the RNA concentration and store at -80 °C for future use.
 7. Follow steps 1.1.6.1 - 1.1.6.5 above for the *EPO* cDNA and mRNA preparation but clone the cDNA into the pCS2⁺ plasmid at EcoRI and XhoI sites instead.
2. Inject Morpholino into zebrafish
 1. Design²³ the MO injections using an online tool (**Table of Materials**) against the ATG sequence of *gata1a*⁴ (5'-CTGCAAGTGTAGATTGAAGATGTC-3') and *tnnt2a*⁵ (5'-CATGTTTGCTCTGATCTGACACGCA-3').
 2. Add *gata1a* and *tnnt2a* MO separately to the nuclease-free water to make the final concentrations of 8 ng/nL and 4 ng/nL, respectively. Repeat with *EPO* mRNA with a final concentration of 20 pg/nL. Ensure that the final volume is 1 mL.
 3. Inject 1 nL of the 8 ng/nL of *gata1a* MO and 1 nL of the 4 ng/nL of *tnnt2a* MO into separate zebrafish embryos at the 1 to the 4-cell stage to reduce ventricular wall shear stress (WSS)²⁴. To increase WSS, inject 1 nL of 20 pg/nL of *EPO* mRNA⁶ into the zebrafish embryos at the 1- to 4- cell stage.
 3. Chemically treat zebrafish to inhibit trabeculation
 1. Using a 20 mL pipette, dilute the 10 mg/mL AG1478 in 1% DMSO in E3 medium to a final concentration of 5 μ M at 30 hpf into a 15 mL tube. As a control, treat each fish with 1% DMSO only.
 2. Add N-[N-(3,5-Difluorophenactyl)-L-Alanyl]-S-Phenylglycine t-butyl ester (DAPT) in 1% DMSO (100 μ M) to E3 medium in a 15 mL tube to inhibit Notch signaling at 40 hpf in a similar fashion. As a control, treat with only 1% DMSO.

2. Imaging Techniques

- 4-D cardiac LSMF Imaging with synchronization algorithm
 - Take 2-D images of the entire fish embryo over multiple cardiac beating cycles using the steps below (**Figure 1**). Ensure that the light-sheet thickness is approximately 5 μm . Take 500 x-y frames with an exposure time of 10 ms. Set the z-scanning to 1 μm for lossless digital sampling according to the Nyquist sampling principle²⁵.
 - Create a 1% (w/v) agarose gel by adding 1 g of agarose to 100 mL and heating it until all agarose is dissolved. Load a small plastic tube with the embryo and agarose using a 20 μL pipette and secure it on the stage.
 - Open the image viewing software and click **Live** to see the live view of the sample. Adjust the objective using the knob so that the sample is in focus. Similarly, move the stage so that the live view of the sample shows the top of the embryo.
 - Take images 500 times for 5 s at 10X magnification using the microscope's software²⁶.
 - Move the stage using the motor to a new layer (1 μm in the z-axis) and repeat the imaging procedure.
 - Repeat above 2 steps until entire heart is fully imaged.

- Ensure data integrity by disregarding the first and last cardiac cycle images. Find the period of the cardiac cycle by matching images that were taken at the same time point in the cardiac cycle, but in different periods. Use the following equation that was developed to find the period:

$$D(z_k, T') = \sum_{m \in Z^2} \sum_{j=1}^{N_z-1} \left\{ \left| I_m[x_m, z_k, \tau_{i(j)}] - I_m[x, z_k, \tau_{i(j)}] \right|^2 + \left| \tau_j' - \tau_{j-1}' \right|^2 / T'^2 \right\}^{1/2} \quad (1)$$

where D is the cost function used for fitting a period hypothesis, I_m the captured image, τ' the time the image was captured, z_k the z-direction index of the image, x_m is the vector of the pixel index, and T' is the periodic hypothesis.

- Use the following equation to find the relative shift between two pictures in similar stages:

$$(s) = \iint_{R^2} \int_0^L |I_m(x, z_k, t) - I_m(x, z_{k'}, t-s)|^2 dt dx \quad (2)$$

where $Q_{k,k'}$ denotes a cost function for the relative shift, R is the possible spatial neighborhood, L is the total time of capturing the image, x is the pixel index, z_k and $z_{k'}$ are the first and second z-direction slices, t is time, and s is the relative shift hypothesis.

- Convert the relative shift to absolute shift with respect to the first image and solve the linear equation using the pseudo-inverse approach, to find the absolute relation to align the next section of images as previously described²⁷.
- The final 4-D images were processed using image processing software (**Table of Materials**).

- Stacking 2-D images into 3-D

- Open a commercial image processing software.
- Click **Open Data**.
- Select all the images to be stacked into 3-D > Click **Load**.
- Add in the voxel size of 0.65 x 0.65 x 1 > Click **OK**.
- Click the **Multi-Planar View** box to visualize the 3-D image.
- Right-click the blue **slice_1.tiff** box > Select **Display** > Select **Volren**.
- Click **Edit** > Select **Options** > Select **Edit Colormap**.
- Adjust the color using the boxes outlined in red > Click **OK**.

- Converting 3-D to 4-D

- Click **File** > Open **Time Series Data**.
- Select the 3-D tiffs that were just made > Click **Load**.
- Enter the same voxel size as before.
- Right click the blue **slice_1.tiff** box > Select **"Display"** > Select **Volren**.
- Click **Edit** > Select **Options** > Select **Edit Colormap**. Adjust the color using the boxes > Click **OK**.
- Right click **Time Series Control** > Click **Movie maker** > Press the **Play** button in order to watch the movie.
- Add a file name, frame size, frame rate, quality equal to 1, type **Monoscopic** > Click **Apply**
- Export the video. Open the video in an appropriate software.

3. qRT-PCR analysis

- Zebrafish heart RNA Isolation to quantify Notch ligands, receptors, and target genes' expressions
 - Sacrifice the zebrafish by subjecting them to an overdose of tricaine methylene^{28,29}. Using a previously described protocol³⁰, the zebrafish hearts were excised and prepared for RNA isolation.
 - Isolate the total RNA, and synthesize the cDNA using the cDNA synthesis kit following the manufacturer's instructions.
 - Design the PCR primers for the Notch ligands *Jag1*, *Jag2*, *Dll4*, receptor *Notch1b*, and signaling related genes *Nrg1* and *ErbB2*. See Table 3 for the primers we used.
 - Add the primers from step 3.1.3, the isolated mRNA from step 3.1.2, and a commercial mastermix to the PCR plate. Run the qRT-PCR at the appropriate temperatures and times according to the enzymes used. Normalize the results to zebrafish α -actin.

Note: This will calculate the expression levels for each of the ligands, receptors, and genes.

4. In vitro Human Aortic Endothelial Cell (HAEC) Experiments

- Dynamic Shear Stress Model

1. Culture HAEC cells with HAEC culture media. Once fully confluent, expose the cells to laminar flow and pulsatile flow of 23×10^{-5} N at the rate of 1 Hz for 24 h.
 1. Warm up EC media/DMEM 10% FBS in a water bath for 20 min.
 2. Retrieve HAEC cells from liquid nitrogen tank and place the vial into the water bath until melted.
 3. Using a 1,000 μ L pipette, remove the thawed cells and put them in a 15 mL tube with 3-5 mL of media. Centrifuge the cell solution at $53 \times g$ for 3 min.
 4. Aspirate the solution off and add enough media for a total volume of 10 mL. Add the cell solution to a sterile T75 flask, cap the flask, and distribute the cells evenly on the bottom of the plate.
 5. Mark the flask with initials, date, cell type, and passage number. Incubate the flask at 37°C , 5% CO_2 , until cells are 80% confluent. Remember to change the media every 2-3 days.
 6. Using a commercial pump, attach the tubing to the flask, and set the parameters mentioned above in step 4.1.1^{31,32,33}.
2. Add GI254023X to 50 mL of HAEC medium at a final concentration of 5 μM for 30 min.
3. With the pre-mixed GI254023X, an ADAM10 inhibitor which suppresses Notch signaling, conduct the same laminar flow or pulsatile flow experiments as in 4.1.1.
4. Quantify Notch ligands (*Jag1*, *Jag2*, and *Dll4*) and Notch target genes (hairless and enhancer of split [*Hes*]) using qRT-PCR for four groups of HAEC samples (laminar flow, laminar flow + GI254023X, pulsatile flow, pulsatile flow + GI254023X) described previously³².

5. Rescue and over-expression of Notch signaling

1. Inject 1 nL of the prepared *Nrg1* mRNA at a concentration of 5 pg/nL (from step 1.1.6) at the 1- to 4-cell stage with the *gata1a* MO in order to overexpress Notch target genes²⁴.
2. Inject 1 nL of the *Nrg1* mRNA into *wea* mutant in a similar way²⁴.
3. Double the concentration of *Nrg1* mRNA (10 pg/nL) and inject²⁴ 1 nL into zebrafish to observe the ventricular morphology.
4. Inject 1 nL of the 20 pg/nL of *EPO* mRNA⁶ into the zebrafish embryos at the 1- to 4- cell stage to augment hematopoiesis to increase ventricular WSS as previously shown²⁴.
5. Inject 1 nL of the 50 μM Isoproterenol⁷, which increases the rate of contractility, to the E3 medium for 24 h while zebrafish are cultured as previously shown²⁴.
6. Perform 4-D LSFM imaging for each group. Follow the instructions in steps 2.1.1-2.1.5.2.8.

6. Quantification of Fractional Shortening and volume change over time

1. Perform 4-D LSFM imaging for each group at 50, 75, and 100 hpf. Follow instructions in steps 2.1.1-2.1.5.2.8. Divide each image so each has 600 nodes for replication of the cardiac wall motion.
2. Measure the change in diameter of the ventricle during diastole and systole using the following formula:

$$\text{Fractional Shortening} = \left(\frac{\text{End diastolic diameter} - \text{End systolic diameter}}{\text{End diastolic diameter}} \right) \times 100 \quad (3)$$
 Load 3-D ventricular images at every 0.1 s with visualization software and measure the volume.
3. Plot the volume change over time for each experimental group at 75 hpf and 100 hpf.

Representative Results

LSFM was used in this manuscript in order to acquire high-resolution 2-D and 3-D pictures. As seen in **Figure 1A** and **1B**, the illumination lens directs the light sheet at the sample. Because of the thinness of the light sheet, only a single plane is illuminated. The detection lens is positioned perpendicular to the illumination lens and is focused on the illuminated plane (**Figure 1B**). The light sheet from the illumination lens then scans the sample from left to right (**Figure 1C**). The scanning allows less photo-bleaching, photo-toxicity, and has a lower signal-to-noise ratio.

LSFM was applied to *Tg(cmlc2a:gfp)* embryos to visualize the entire cardiac structure³⁴ by rapid scanning (> 30 s) with a voxel resolution of $0.65 \times 0.65 \times 1 \mu\text{m}$. Due to a single plane illumination, background noise was significantly reduced (**Figure 1**). Trabecular ridges protruded into the ventricular lumen at 75 hpf, and a trabecular network clearly was shown at 100 hpf (**Figure 2A, B**). *Gata1a* MO micro-injection reduced hematopoiesis and viscosity by 90%^{4,35}. This decreased viscosity attenuated hemodynamic shear stress, resulting in a delayed initiation and density of trabecular network at 75 hpf and 100 hpf when compared to control group (**Figure 2C, D**). Furthermore, Notch ligands (*Dll4*, *Jag1*, and *Jag2*), receptor (*Notch1b*), and downstream signaling components (*Nrg1* and *ErbB2*) were down-regulated in response to *gata1a* MO injection ($p < 0.05$, $n=5$) (**Figure 2K**)^{2,8,36}. Co-injection of *gata1a* MO with 5 μM of *Nrg1* mRNA up-regulated Notch signaling-related gene expression and rescued trabecular formation at 75 hpf and 100 hpf (**Figure 2E, F, K**). Thus, *gata1a* MO reduced hemodynamic forces leading to down-regulation of Notch signaling, whereas *Nrg1* mRNA rescue up-regulated Notch-related genes and re-initiated trabeculation.

In order to further prove our hypothesis that changing hemodynamic forces and thus trabeculation via Notch signaling, we introduced the *wea* mutant that develops a non-contractile atrium³⁷. In the absence of ventricular inflow and hemodynamic forces during atrial systole, *wea* mutants express lower cardiac mRNA levels of Notch signaling component genes and target genes compared to controls, and harbor non-trabeculated, small and weakly contracting ventricles (**Figure 2G, L**). However, *Nrg1* mRNA micro-injection into the *wea* mutants up-regulated the Notch signaling pathway, accompanied by the partial rescue of trabecular ridges, leading to a more pronounced contractile ventricle despite a non-contractile atrium (**Figure 2H, L**)². In this context, the *wea* mutants corroborated the relation between the non-contractile atrium and a non-trabeculated ventricle, underscoring the hemodynamic modulation of trabeculation via Notch signaling.

Tnnt2a MO was delivered to stop cardiac contraction by inhibiting cardiac troponin T^{38,39}. The *tnnt2a* MO-injected fish were completely devoid of circulation and ventricular WSS due to significant down-regulated Notch signaling, leading to a smooth ventricular surface and thin wall when compared to control group (Figure 2I, M). To investigate whether WSS on the endocardium was a requirement for trabeculation, we also have *cloche* (*clo*) mutants for which endocardium and the endothelial lining of the heart do not develop^{40,41}. The *clo* mutant failed to develop cardiac trabeculae and showed smaller sized ventricle and incomplete cardiac looping (Figure 2J). Thus, the endocardial lining is necessary to sense hemodynamic shear stress to activate Notch signaling (Figure 2M). However, when the hemodynamic shear stress was increased by increasing hematopoiesis or treatment of isoproterenol to increase contractility, the expression levels of Notch-related genes did not increase, and the trabecular network morphology did not change (Figure 3).

To further demonstrate the relationship between shear stress and Notch signaling, HAECs were used for *in vitro* tests. A pulsatile flow was exerted on confluent cells to simulate the hemodynamic shear stress observed by endothelial cells. It is shown that compared to static culture, pulsatile culture increases expression of Notch-related genes (Figure 4). Furthermore, treatment with the ADAM10 inhibitor significantly reduced Notch signaling (Figure 4).

Next, we calculated ventricular fractional shortening, and ventricular cavity change in volume over time for the wild-type, *gata1a* MO, AG1478, and those rescued by *Nrg1* injection groups at 50 hpf, 75 hpf, and 100 hpf (Figure 5A-C). Treatment with *ErbB* signaling inhibitor, AG1478, significantly delayed and reduced fractional shortening during ventricular diastole at 100 hpf (Figure 5A). Both *gata1a* MO and AG1478 treatment reduced ventricular chamber size during contraction, as assessed by the changes in 4-D LSFM (Figure 5E, F). Both groups developed an increased end-systolic and -diastolic volume when compared to the wild-type. Co-injection of *Nrg1* mRNA with *gata1a* MO restored both fractional shortening, and Ejection Fraction toward those of the wild type.

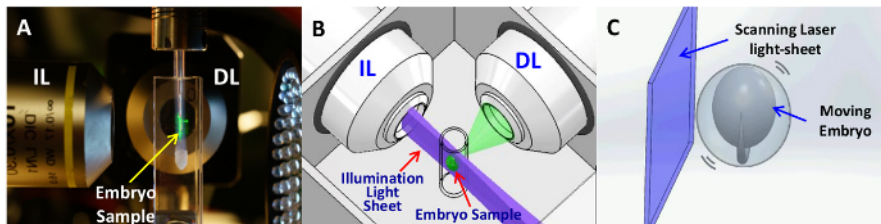


Figure 1: Fluorescent light sheet overview. (A) Representative LSFM system where the sample is placed in the intersection of the light sheet from the illumination lens (IL) and the detection path of the detection lens (DL). (B) The cylindrical lens behind the IL creates the micron-sized light sheet (purple) within the sample, which excites a thin sheet of the sample. The detection lens records the emitted fluorescent signal. (C) A schematic of the thin laser sheet (purple) optically sectioning the zebrafish embryo which moves right to left. This figure has been modified from Lee *et al*¹⁷. Please click here to view a larger version of this figure.

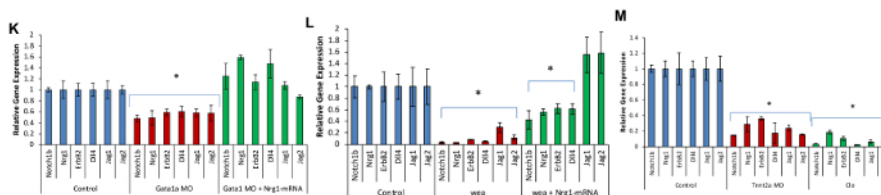
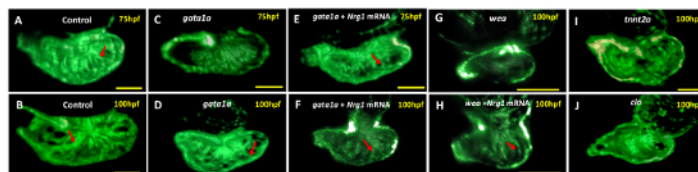


Figure 2: Ventricular morphologies of genetically manipulated *Tg(cmlc:gfp)* zebrafish with Notch Ligand, receptor, and target gene expression. (A) The trabecular network is shown at 75 hpf of control zebrafish. (B) The trabecular network at 100 hpf of control zebrafish. (C) Injection of *gata1a* MO at the 1- to 4-cell stage showed little to no trabeculation at 75 hpf. (D) Injection of *gata1a* MO into zebrafish had delayed trabecular network formation. (E) Co-injection of *gata1a* MO and human *Nrg1* mRNA partially restored trabeculation at 75 hpf. (F) Co-injection of *gata1a* MO and human *Nrg1* mRNA almost completely restored the trabecular network at 100 hpf. (G) *wea* mutant at 100 hpf shows no trabeculation and a smooth ventricular wall. (H) Injection of human *Nrg1* into *wea* mutant zebrafish partially restored trabeculation at 100 hpf. (I) Injection of *tnnt2a* MO showed no trabeculation at 75 hpf (not shown) and 100 hpf. (J) *clo* mutant showed no trabeculation at 100 hpf. (K) Injection of the *gata1a* MO significantly reduced mRNA expression of *Notch1*, *Nrg1*, and *Jag2* (t-test, **P* < 0.05, n=5 vs. control). Co-injection of *gata1a* MO and human *Nrg1* mRNA significantly increased the expression of *Notch1b*, *Nrg1*, *ErbB*, and *Jag1* compared to control. (L) The *wea* mutant had the significantly lower expression of Notch-related genes (t-test, **P* < 0.05, n=5 vs. control). Injection of human *Nrg1* increased the expression of Notch-related genes; *Jag1* and *Jag2* were significantly higher than control. (M) The *tnnt2a* MO injection and *clo* mutant showed a significantly lower expression of Notch-related genes (t-test, **P* < 0.05, n=5 vs. control). Scale bars: 50 μ m. Data are shown as the mean standard deviation. This figure has been modified from Lee *et al*¹⁷. Please click here to view a larger version of this figure.

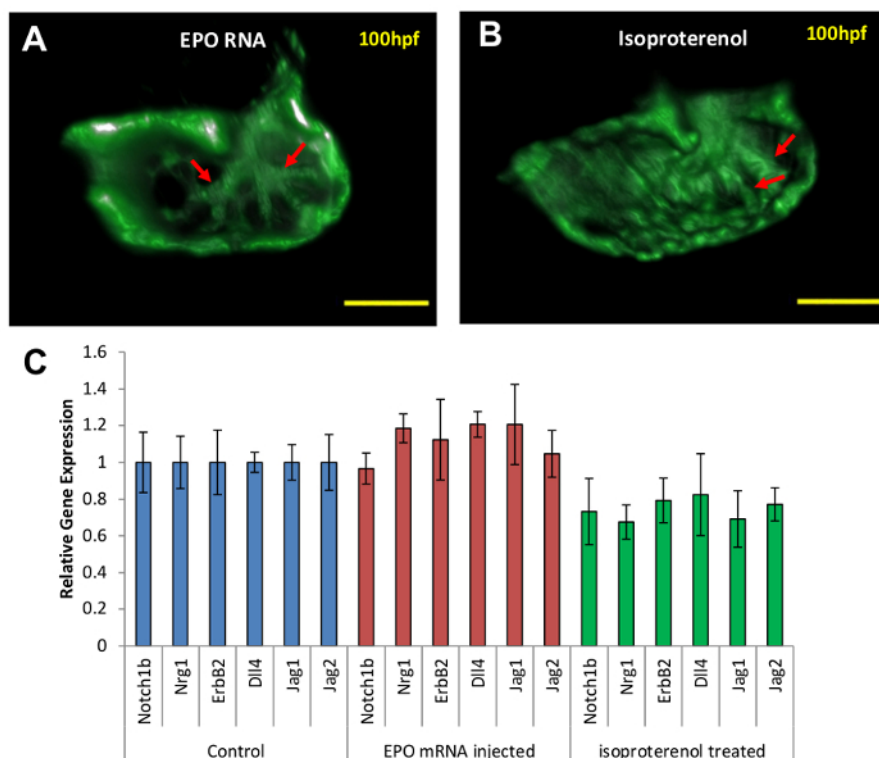


Figure 3: Increasing WSS in manipulated *Tg(cmlc:gfp)* zebrafish with Notch ligand, receptor and target gene expression *in vivo*. Increasing the WSS via over-expression of hematopoiesis with the injection of *EPO*(A) or addition of ISO (B) via increasing heart rate did not increase trabeculation and had a trabecular network similar to that of the control. (C) The injection of *EPO* mRNA or Isoproterenol did not change the expression of Notch ligand, receptor or target genes (t-test, *P < 0.05, n=5 vs. control). This figure has been modified from Lee *et al*¹⁷. [Please click here to view a larger version of this figure.](#)

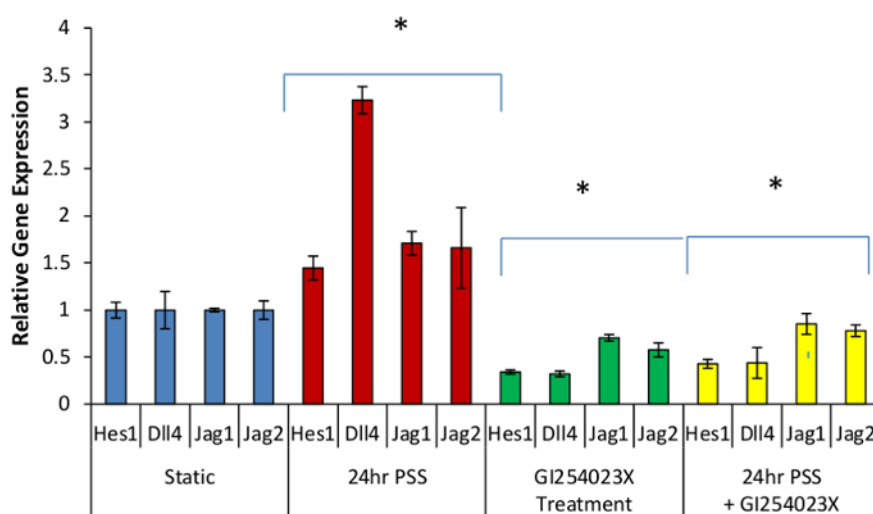


Figure 4: Endothelial cells subject to oscillatory or pulsatile shear stress *in vitro*. HAECs subject to the pulsatile shear stress of $\tau_{\text{average}} = 30 \times 10^{-5}$ N/s at 1 Hz had upregulated Notch-related gene expressions and downregulated of Notch-related gene expressions when the ADAM10 inhibitor was applied (t-test, *P < 0.05, n=5 vs. control). This figure has been modified from Lee *et al*¹⁷. [Please click here to view a larger version of this figure.](#)

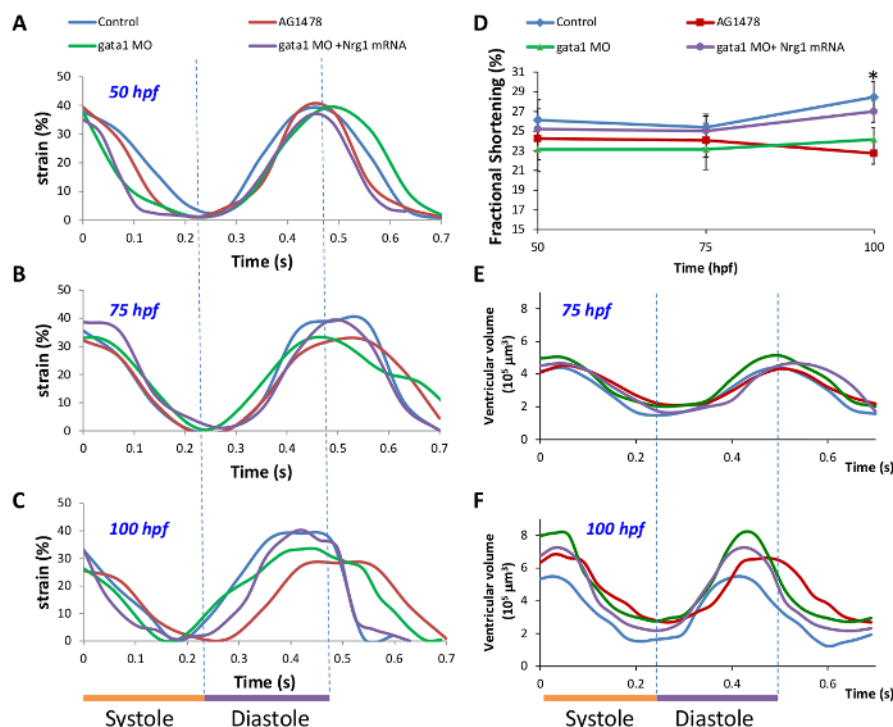


Figure 5: Effect of trabeculation of fractional shortening and ejection fraction. (A-C) Addition of AG1478 and *gata1a* MO significantly decreased the fractional shortening at 100 hpf, but co-injection of human *Nrg1* and *gata1a* MO improved it. (D) *gata1a* injection and AG1478 significantly decreased the fractional shortening at 100 hpf (t-test, *P < 0.05, n=5 vs. control). Co-injection of *gata1a* and *Nrg1* mRNA improved the fractional shortening. (E-F) Integrating the 4-D synchronization algorithm with LSMF showed that AG1478 and *gata1a* MO had increased end systolic and diastolic volumes at 75 hpf (E) and 100 hpf (F). Data are shown as the mean standard deviation. This figure has been modified from Lee *et al*¹⁷. Please click here to view a larger version of this figure.

Zebrafish Jag1	Forward	CCGCGTATGTTTGAAGGAGTATCAGTCG
	Backward	CAGCACGATCCGGGTTTTGTCTG
Zebrafish Jag2	Forward	AGCCCTAGCAAAACGAGCGACG
	Backward	GCGTGAATGTGCCGTTTCGATCAA
Zebrafish Dll4	Forward	CAAAGTGGAAGCAGACAGAGCTAAGG
	Backward	CGGTCAATCCCTGGGTGTGCATT
Zebrafish BMP10	Forward	GCATCAAGGGGCCACTCGTGTAGA
	Backward	TCGTCTCACTCCACTAGGTCCCATACTG
Zebrafish ErBb2	Forward	GATCAGGACTGCCAAACATTGACGTCT
	Backward	AGCAGCACACTGAACATGGCAGCA
Zebrafish Nrg-1	Forward	GTGTGTTTGTCCCTGTGGACGCGT
	Backward	CCTCCTGGAGCTTCCCCTCAAACA
Zebrafish Notch1b	Forward	CAGAGAGTGAGGCACAGTGCAATCC
	Backward	GCCGTCCCATTCACTCTGCATT

Table 3: Primers used for Zebrafish screening.

Discussion

In this protocol, we have shown that 4-D imaging can be used to track the development of a trabecular network in response to changes in biomechanical forces. In particular, the shear stress experienced by endothelial cells initiates the Notch signaling cascade, which in turn promotes trabeculation. In this manuscript, we have shown that (1) *gata1a* MO injection decreased hematopoiesis and therefore it reduced wall shear stress, (2) *tnnt2a* MO injection inhibited ventricular contractile function to reduce wall shear stress, and (3) *wea* mutants lacked atrial contraction, which then decreased the hemodynamic force applied to the ventricle. By reducing the shear stress on the cardiac walls, we quantified the Notch signaling via qRT-PCR and found that with reduced WSS, there was reduced Notch signaling. To further prove our

hypothesis, *c/o* mutants that lacked endocardium did not form trabeculae, and subjecting endothelial cells to pulsatile shear stress with ADAM10 present showed that shear stress activates Notch signaling.

The other imaging techniques such as confocal microscopy can be used to image samples in 3-D¹⁴. However, this technique and others have many drawbacks. For example, the confocal imaging cannot penetrate deeply into samples, has the low axial resolution, and slow scanning speeds^{19,42}. Because of the penetration depth limit in confocal imaging, small samples, such as zebrafish embryos, can only be imaged in its entirety. Two-photon confocal microscopy improves the penetration depth, but the resolution, slow scanning speed, and high cost make this technique undesirable¹³. There have been studies that combine two-photon microscopy and LSFM successfully¹⁸, however, the drawbacks are still prominent⁴².

LSFM, on the other hand, has the least photo-bleaching and damage^{13,18,42}, fast acquisition speed, and similar penetration depth¹³. Additionally, because of the dual lenses and excitation of a single plane (**Figure 1**), the background noise is substantially reduced⁴³. However, the samples need to be embedded into gels to immobilize the sample, which makes it difficult to apply to *in vivo* models other than zebrafish^{14,17,19}. Also, utilization of the fluorescent light limits the depth penetration to a few millimeters. Even though LSFM is a great method for visualization, it is critical that it is supplemented with quantitative data. Because LSFM is only qualitative, it can be subject to various interpretations. Using qRT-PCR, we could confirm that the LFSM 4-D images were a correct representation of the events occurring in the live samples. Occasionally in larger samples, stripes and shadows can form in the images. However, dual-sided illumination or mSPIM can be utilized to reduce these artifacts⁴². Because LSFM is so versatile, its capability of capturing high resolution and overall better-quality images makes the future of LSFM promising. Mentioned previously, LSFM can be combined with other imaging systems for successful imaging^{18,42}.

We demonstrated previously that applying a pulsatile shear stress of 23×10^{-5} N at 1 Hz for 24 h substantially upregulates Notch signaling *in vitro* (**Figure 4**)¹⁷. We further demonstrated that shear forces activate Notch signaling by genetic manipulation of hematopoiesis (*gata1a* MO)⁴, cardiac contraction (*tnnt1a* MO)⁵, atrial contraction (*wea* mutant), endocardial deletion (*c/o* mutant), and localization of Notch signaling (*Tgflk:mCherry;tp1:gfp*). We describe here that by lowering the wall shear stress in the ventricle, that Notch-related genes were down-regulated (**Figure 2K, L, M**). Furthermore, we were able to demonstrate that *Nrg1* mRNA was able to rescue trabeculation, restore Notch signaling, and improve ventricular fractional shortening and ejection fraction (**Figure 2E, F, H, K-M, Figure 5**). The restoration of cardiac function was shown by the increase in contractile function-mediated hemodynamic forces that activated Notch signaling (**Figure 2K-M**).

We also determined that the shear stress-activated Notch signaling is endocardial dependent. By using *gata1a* MO, *tnnt2a* MO, *wea* mutant or AG1478 treatment, trabeculation was inhibited and Notch signaling was down-regulated (**Figure 2K-M**). However, *Nrg1* rescued trabeculation and Notch signaling in *wea* mutants and when co-injected with *gata1a* MO (**Figure 2D, H, K, L**). When wall shear stress (*EPO* injection) or Notch signaling (10 pg/nL *Nrg1* injection) was increased, there was no change in the *EPO* group in terms of morphology, but abnormal ventricular morphogenesis was present in the *Nrg1* increased dose (**Figure 3**).

In conclusion, we have shown that the mechanotransduction of shear stress activates the Notch signaling pathway. By applying 4-D LSFM and genetically engineered zebrafish, we developed a new model system that shows how critical blood flow is during cardiac development to its morphology, contractility, and overall function.

Disclosures

The authors have nothing to disclose.

Acknowledgements

The authors would like to express gratitude to William Talbot from Stanford University for providing the Human *Nrg1* cDNA and to Deborah Yelon from UCSD for providing the *wea* mutants. The authors would also like to thank Cynthia Chen for helping with image acquisition. This study was supported by grants NIH HL118650 (to T.K. Hsiai), HL083015 (to T.K. Hsiai), HD069305 (to N.C. Chi and T.K. Hsiai.), HL111437 (to T.K. Hsiai and N.C. Chi), HL129727 (to T.K. Hsiai), T32HL007895 (to R.R. Sevag Packard), HL 134613 (to V. Messerschmidt) and University of Texas System STARS funding (to J. Lee).

References

1. Lee, J. *et al.* Moving domain computational fluid dynamics to interface with an embryonic model of cardiac morphogenesis. *PLoS One*. **8** (8), e72924 (2013).
2. Peshkovsky, C., Totong, R., & Yelon, D. Dependence of cardiac trabeculation on neuregulin signaling and blood flow in zebrafish. *Dev Dyn*. **240** (2), 446-456 (2011).
3. High, F. A., & Epstein, J. A. The multifaceted role of Notch in cardiac development and disease. *Nat Rev Genet*. **9** (1), 49-61 (2008).
4. Galloway, J. L., Wingert, R. A., Thisse, C., Thisse, B., & Zon, L. I. Loss of Gata1 but Not Gata2 Converts Erythropoiesis to Myelopoiesis in Zebrafish Embryos. *Developmental Cell*. **8** (1), 109-116 (2005).
5. Chi, N. C. *et al.* Cardiac conduction is required to preserve cardiac chamber morphology. *Proceedings of the National Academy of Sciences*. **107** (33), 14662 (2010).
6. Paffett-Lugassy, N. *et al.* Functional conservation of erythropoietin signaling in zebrafish. *Blood*. **110** (7), 2718 (2007).
7. De Luca, E. *et al.* ZebraBeat: a flexible platform for the analysis of the cardiac rate in zebrafish embryos. *Scientific Reports*. **4** 4898, (2014).
8. Liu, J. *et al.* A dual role for ErbB2 signaling in cardiac trabeculation. *Development*. **137** (22), 3867-3875 (2010).
9. Samsa, L. A. *et al.* Cardiac contraction activates endocardial Notch signaling to modulate chamber maturation in zebrafish. *Development*. **142** (23), 4080-4091 (2015).
10. Li, Y. *et al.* Global genetic analysis in mice unveils central role for cilia in congenital heart disease. *Nature*. **521** 520, (2015).

11. Sifrim, A. *et al.* Distinct genetic architectures for syndromic and nonsyndromic congenital heart defects identified by exome sequencing. *Nature Genetics*. **48** 1060, (2016).
12. Hu, Z. *et al.* A genome-wide association study identifies two risk loci for congenital heart malformations in Han Chinese populations. *Nature Genetics*. **45** 818, (2013).
13. Huisken, J., & Stainier, D. Y. R. Selective plane illumination microscopy techniques in developmental biology. *Development (Cambridge, England)*. **136** (12), 1963-1975 (2009).
14. Panier, T. *et al.* Fast functional imaging of multiple brain regions in intact zebrafish larvae using Selective Plane Illumination Microscopy. *Frontiers in Neural Circuits*. **7** 65 (2013).
15. Lee, E. *et al.* ACT-PRESTO: Rapid and consistent tissue clearing and labeling method for 3-dimensional (3D) imaging. *Scientific Reports*. **6** 18631, (2016).
16. Kelley, L. C. *et al.* Live-cell confocal microscopy and quantitative 4D image analysis of anchor-cell invasion through the basement membrane in *Caenorhabditis elegans*. *Nature Protocols*. **12** 2081, (2016).
17. Lee, J. *et al.* 4-Dimensional light-sheet microscopy to elucidate shear stress modulation of cardiac trabeculation. *The Journal of Clinical Investigation*. **126** (5), 1679-1690 (2016).
18. Lavagnino, Z. *et al.* 4D (x-y-z-t) imaging of thick biological samples by means of Two-Photon inverted Selective Plane Illumination Microscopy (2PE-iSPIM). *Scientific Reports*. **6** 23923, (2016).
19. Huisken, J., Swoger, J., Del Bene, F., Wittbrodt, J., & Stelzer, E. H. K. Optical Sectioning Deep Inside Live Embryos by Selective Plane Illumination Microscopy. *Science*. **305** (5686), 1007 (2004).
20. Hove, J. R. *et al.* Intracardiac fluid forces are an essential epigenetic factor for embryonic cardiogenesis. *Nature*. **421** (6919), 172-177 (2003).
21. Bakkers, J. Zebrafish as a model to study cardiac development and human cardiac disease. *Cardiovascular Research*. **91** (2), 279-288 (2011).
22. BioRad. *General Protocol for Western Blotting*. **6376**, http://www.bio-rad.com/webroot/web/pdf/lsr/literature/Bulletin_6376.pdf (2018).
23. GeneTools. *Gene Tools Oligo Design Website*. <https://oligodesign.gene-tools.com/request/> (2018).
24. Mullins, M. in *Zebrafish Course*. (ed University of Chicago) (2013).
25. Grenander, U. *Probability and Statistics: The Harald Cramér Volume*. Alqvist & Wiksell, (1959).
26. Fei, P. *et al.* Cardiac Light-Sheet Fluorescent Microscopy for Multi-Scale and Rapid Imaging of Architecture and Function. *Scientific Reports*. **6** 22489, (2016).
27. Liebling, M., Forouhar, A.S., Gharib, M., Fraser, S.E., Dickinson M.E. Four-dimensional cardiac imaging in living embryos via postacquisition synchronization of nongated slice sequences. *Journal of Biomedical Optics*. **10**, (5) (2005).
28. Adeoye, A. A. *et al.* Combined effects of exogenous enzymes and probiotic on Nile tilapia (*Oreochromis niloticus*) growth, intestinal morphology and microbiome. *Aquaculture*. **463** 61-70 (2016).
29. Matthews, M., & Varga, Z. M. Anesthesia and Euthanasia in Zebrafish. *ILAR Journal*. **53** (2), 192-204 (2012).
30. Singleman, C., & Holtzman, N. G. Heart Dissection in Larval, Juvenile and Adult Zebrafish, *Danio rerio*. *Journal of Visualized Experiments : JoVE*. (55), e3165 (2011).
31. Li, R. *et al.* Disturbed Flow Induces Autophagy, but Impairs Autophagic Flux to Perturb Mitochondrial Homeostasis. *Antioxidants & Redox Signaling*. **23** (15), 1207-1219 (2015).
32. Li, R. *et al.* Shear Stress-Activated Wnt-Angiopoietin-2 Signaling Recapitulated Vascular Repair in Zebrafish Embryos. *Arteriosclerosis, thrombosis, and vascular biology*. **34** (10), 2268-2275 (2014).
33. Baek, K. I. *et al.* Flow-Responsive Vascular Endothelial Growth Factor Receptor-Protein Kinase C Isoform Epsilon Signaling Mediates Glycolytic Metabolites for Vascular Repair. *Antioxidants & Redox Signaling*. **28** (1), 31-43 (2018).
34. Huang, C.-J., Tu, C.-T., Hsiao, C.-D., Hsieh, F.-J., & Tsai, H.-J. Germ-line transmission of a myocardium-specific GFP transgene reveals critical regulatory elements in the cardiac myosin light chain 2 promoter of zebrafish. *Developmental Dynamics*. **228** (1), 30-40 (2003).
35. Vermot, J. *et al.* Reversing blood flows act through *klf2a* to ensure normal valvulogenesis in the developing heart. *PLoS Biol.* **7** (11), e1000246 (2009).
36. Grego-Bessa, J. *et al.* Notch signaling is essential for ventricular chamber development. *Dev Cell*. **12** (3), 415-429 (2007).
37. Berdugo, E., Coleman, H., Lee, D. H., Stainier, D. Y. R., & Yelon, D. Mutation of weak atrium/atrial myosin heavy chain disrupts atrial function and influences ventricular morphogenesis in zebrafish. *Development*. **130** (24), 6121 (2003).
38. Arnaout, R. *et al.* Zebrafish model for human long QT syndrome. *Proc Natl Acad Sci U S A*. **104** (27), 11316-11321 (2007).
39. Chi, N. C. *et al.* Genetic and physiologic dissection of the vertebrate cardiac conduction system. *PLoS Biol.* **6** (5), e109 (2008).
40. Liao, W. *et al.* The zebrafish gene *cloche* acts upstream of a *flk-1* homologue to regulate endothelial cell differentiation. *Development*. **124** (2), 381-389 (1997).
41. Stainier, D. Y., Weinstein, B. M., Detrich, H. W., 3rd, Zon, L. I., & Fishman, M. C. *Cloche*, an early acting zebrafish gene, is required by both the endothelial and hematopoietic lineages. *Development*. **121** (10), 3141-3150 (1995).
42. Santi, P. A. Light Sheet Fluorescence Microscopy: A Review. *Journal of Histochemistry and Cytochemistry*. **59** (2), 129-138 (2011).
43. Engelbrecht, C. J., & Stelzer, E. H. Resolution enhancement in a light-sheet-based microscope (SPIM). *Optics Letters*. **31** (10), 1477-1479 (2006).